Two-Photon Absorption and First Nonlinear Optical Properties of Ionic Octupolar Molecules: Structure−Function Relationships and Solvent Effects

Paresh Chandra Ray* and Jerzy Leszczynski

Department of Chemistry, Jackson State University, Jackson, Mississippi 39217

Received: January 7, 2005; In Final Form: April 30, 2005

We present a quantum-chemical analysis of the two-photon absorption properties and first hyperpolarizabilities of a series of ionic octupolar molecules and a comparison of their characteristics with corresponding neutral molecules. The molecular geometries are obtained via BL3YP/6-31G (d,p) level optimization including the SCRF/PCM approach, while the dynamic NLO and two-photon absorption properties are calculated with the ZINDO/CV method including solvent effects. The effects of donor or acceptor substitution and elongation of the conjugation path length are established to demonstrate the engineering guidelines for enhancing two-photon absorption cross section and molecular optical nonlinearities. It is found that the chain length dependence of the two-photon absorption and the first nonlinearity follow the same trend, displaying a saturation limit at $n = 5$. The solvent induced effect on the two-photon absorption and NLO properties are studied using the ZINDO/CV/SCRF method. It has been observed that two-photon absorption and the first nonlinearity peaks at $\epsilon \approx 20$ and then decreases slightly, approaching saturation. We also compare our theoretical findings with the experimental results wherever available in the literature.

Introduction

Photonics is playing an ever-increasing role in our modern information society. It is gradually replacing electronics. In recent years, an intense worldwide effort has been focused on the research of design and development of organic conjugated materials with large optical nonlinearities due to their potential applications in various optical devices.[1−5] Materials with high nonlinear optical (NLO) activities are useful as electro-optic switching elements for telecommunication and optical information processing. A large number of organic π-conjugated molecules have been investigated in the last 20 years.[1−5] The outcome of such studies has helped to establish certain guidelines for molecular design of the second-order nonlinear optical materials with desired properties. However, roughly more than 80% of all π-conjugated organic molecules crystallize in centrosymmetric space groups, therefore producing materials with no second-order bulk susceptibility, $\chi(2)$. To overcome this problem, ionic and octupolar organic chromophores are considered to be an important class of materials for applications in second-order nonlinear optics.[5−9]

Zyss et. al.[9−11] recognized in the early 1990s that the inherent conflict between dipole minimization and molecular hyperpolarizability is not essential. It could be ultimately resolved by enlarging the pool of candidate molecules to encompass non-centrosymmetric systems known as octupoles. For such systems, their symmetry ensures cancellation of their dipole moment as well as of any other physical property behaving like a vector under symmetry operations. A common way to design second-order NLO-active octopolar molecules is to develop non-centrosymmetrically substituted trigonal or tetrahedral π-conjugated systems that display efficient charge transfer from the periphery to the center of the molecule. Octupolar molecules with the 3-fold symmetry have several advantages in comparison to the more conventional dipolar molecules, and these are the following: (i) The molecular hyperpolarizabilities of octupoles increase monotonically with the extent of charge transfer.[14−18] Therefore, to obtain octupolar molecules with large β, one needs to increase the D−A strength, conjugation length, and π orbital energy. (ii) It has already been demonstrated[15,16] that two-dimensional octupoles usually produce non-centrosymmetric crystals spontaneously. Moreover, such crystals show no sign of phase transition relaxation for a prolonged period of time, probably due to the lack of the ground-state molecular dipole moment. This phenomenon suggests that a new crystal engineering principle could be developed for the production of electro-optic material based on octupolar molecules with a large bulk nonlinearity. (iii) The second harmonic response of octupolar molecules does not depend on the polarization unlike dipolar compounds and therefore has important implications for applications. (iv) It has been demonstrated[14−16] that octupolar molecules exhibit 3−8 times higher first hyperpolarizabilities than the corresponding dipolar derivatives. Recent studies have highlighted the potential of both metal-containing[15−17] and particularly organic compounds as octupolar quadratic NLO materials.[9−14,18−20]

We have already shown[13] experimentally that the symmetrically substituted triazines have larger first hyperpolarizabilities than their corresponding benzene analogues. Zhu et al.[21] have investigated theoretically the first hyperpolarizabilities of a series of octupolar triazines containing a wide variety of the five-membered aromatic heteroines by using the RHF/6-31G level molecular orbital method. Cho et al.[14] have reported 1,3,5-tricyano-2,4,6-tris(vinyl) benzene derivatives with very large second-order nonlinear optical properties. However, there is only one report on the ionic octupolar NLO systems based on 1,3,5-substituted aromatic rings, and that is from our group. Due to their ionic interaction, they conquer the dipole attraction, and in fact, ionic dipolar compounds exhibit excellent bulk second

10.1021/jp050117f CCC: $30.25
Published on Web 07/13/2005

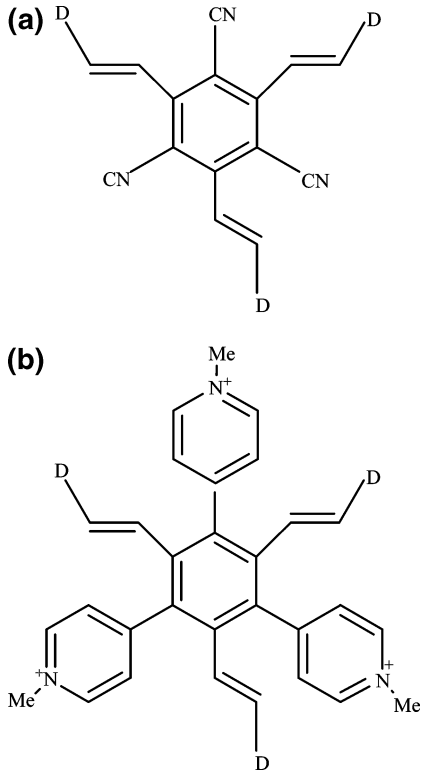

Figure 1. (a) Structure of the neutral octupolar molecule used in this study. (b) Structure of the ionic octupolar molecule used in this study.

harmonic generation efficiency.[1−4] Recently,[22−24] we have shown that the ionic dipolar and octupolar chromophores have several times larger β than the analogous electrically neutral molecules.

By two-photon absorption (TPA), a molecule is excited from the ground state to the excited state by simultaneous absorption of two photons. TPA has the advantage of high transmission at low incident intensity for incident light with an optical frequency below the band gap frequency. In recent years, there has been growing interest in the design and synthesis of organic nonlinear optical materials with large TPA cross-section values due to their potential application in power limiting,[25] up-conversion lasing,[26] three-dimensional fluorescence imaging,[27] pulse reshaping and stabilization,[28] photodynamic therapy,[29] three-dimensional optical data storage,[30] and microfabrication.[31] The development of the two-photon technology depends much on the success of designing new molecules with large TPA cross sections at desirable wavelengths. It is found that[32−34] the molecular structure has a significant influence on the TPA cross section of a molecule. Therefore, the study of the relationship between molecular geometry and the TPA cross section is quite important. Various design strategies have been employed to enhance the magnitude of the TPA cross section of dyes.[32−42] However, to the best of our knowledge, mostly dipolar molecules have been investigated.[32−37] Studies on the TPA properties of multidimensional (octupolar) systems are very few.[38,42−44] In addition, there are no attempts to design ionic octupolar TPA systems.

In this paper, we report a systematic study of the design criteria for the ionic octupolar systems. We have investigated the first hyperpolarizabilities and TPA properties of a series of 1,3,5-substituted aromatic ionic octupoles (Figures 1 and 2a and b) using a combination of density functional theoretical (DFT) calculations with the 6-31G (d,p) basis set and the ZINDO/CV method. We have also compared the results with corresponding neutral octopolar molecules. 1,3,5-Substituted aromatic octupoles can exist in four different forms in the ground state, and these are the valence-bond (VB) state and three types of charge-transfer (CT) states, as shown in Figure 2c. Contribution of each form to the total ground-state configuration varies with solvent, donor−acceptor parameters, and conjugation. Thus, the CT character of the ground states varies with the different parameters as we discussed above. To understand how the solvent polarity affects the structure of the octupolar molecules, we have used the self-consistent reaction field (SCRF) approach with the polarizable continuum model (PCM).[45] To account for both solvent and dispersion effects, we have adapted the ZINDO/CV technique with the SCRF method for the calculation of β.

Computational Method

The molecular geometries of all of the molecules reported in this paper have been fully optimized at the B3LYP (DFT) level with the 6-31G (d,p) basis set using the Gaussian 03 program. To explicitly take into account the solvent polarity effects, we have adapted the self-consistent reaction field (SCRF) approach with the polarizable continuum model (PCM)[45] as implemented in Gaussian 03.[46] The PCM model represents a molecular solute as a quantum mechanical charge distribution contained in a molecular cavity. The cavity is assumed to be immersed in a continuum dielectric. When the dielectric is polarized by the solute, the induced separation of charge gives rise to a response field that modifies the previous state of the solute charge distribution. The radius of the molecular-shape cavity used for this DFT/PCM calculation was determined from the molecular length + van der Waals radius of the outermost atoms. To calculate dynamic β values, we have adapted the ZINDO/CV technique combined with the SCRF method. The primary code for the ZINDO algorithm was developed by Zerner and coworkers,[47] while the ZINDO/SOS technique has been extensively used by several authors to compute β for different molecules.[48,49] Recently, the ZINDO method has been combined with the correction vector techniques to obtain dynamic NLO coefficients in which the sum over all the eigenstates of the chosen configuration interaction (CI) Hamiltonian is exactly included.[22,23,50,51] We have used this technique to calculate β for the ionic and neutral weak organic acids,[51] and the theoretical values match very well with the experimental data obtained via the HRS technique. The ZINDO calculation of first hyperpolarizabilities follows the correction vector methods as described by Ramasesha et. al.[50] In this method, we can obtain the NLO coefficients without resorting to the usual procedure of explicitly solving for a large number of excited states of the CI Hamiltonian, followed by a computation of the transition dipoles among these states. The first-order CV, $\phi_i^{(1)}(\omega)$, is defined by the inhomogeneous linear algebraic equation

$$(\mathbf{H} - E_G + \hbar\omega + i\Gamma)\phi_i^{(1)}(\omega) = \mu_i|G\rangle \qquad (1)$$

where **H** is the CI Hamiltonian matrix in the chosen many-body basis, E_G is the ground-state energy, ω is the frequency, $\mu_i = \mu_i = \langle G|\mu_i|G\rangle$ is the ith component of the dipole displacement operator ($i = x, y, z$), and h/Γ is the average lifetime of the excited states. It can be shown that $\phi_i^{(1)}(\omega)$, if expressed on the basis of the eigenstates, $\{|R\rangle\}$, of the CI

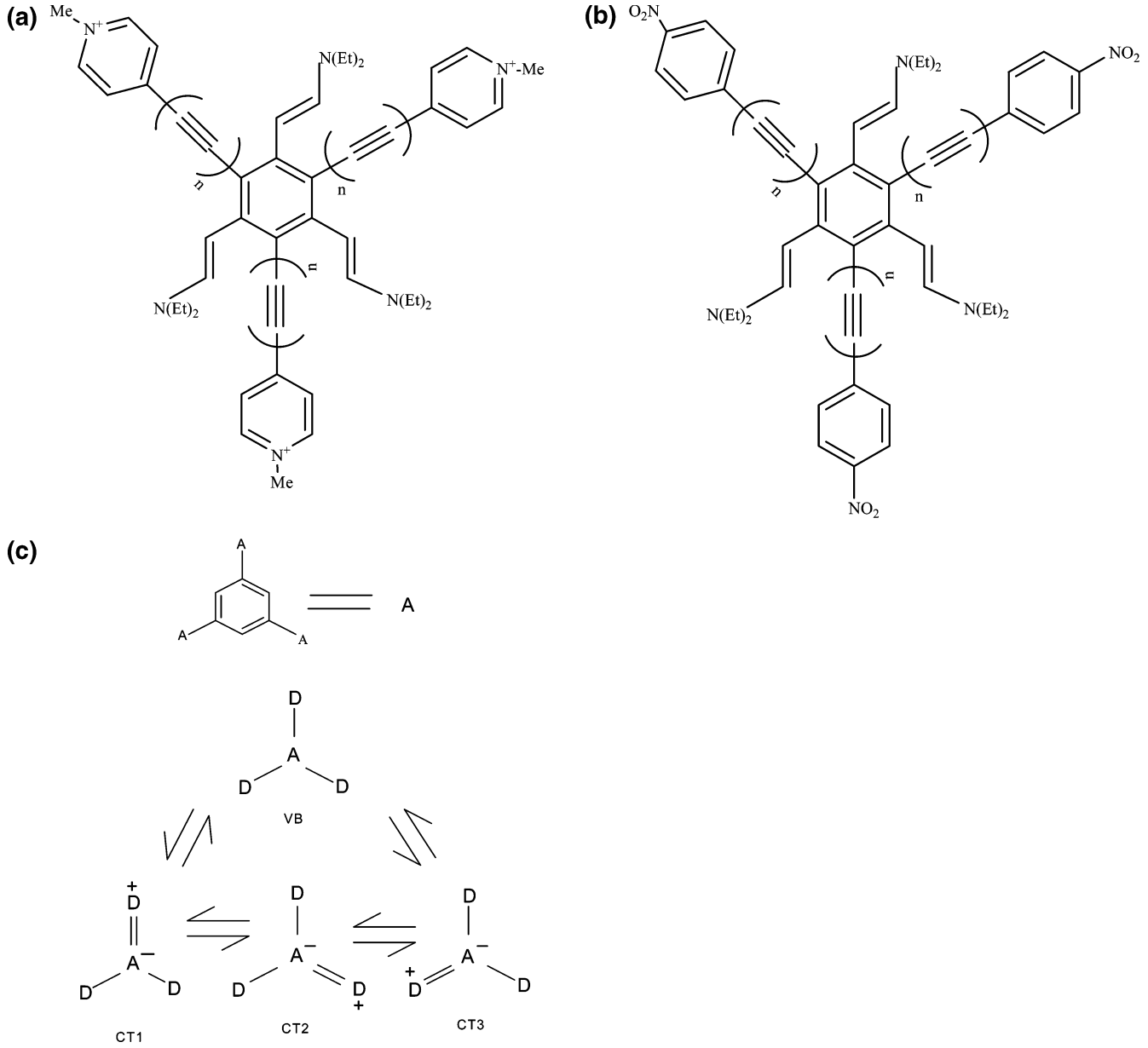

Figure 2. (a) Structure of the extended conjugated ionic octupolar molecule used in this study. (b) Structure of the extended conjugated neutral octupolar molecule used in this study. (c) Schematic representation of the three possible charge-transfer structures of the octupolar molecules considered in this manuscript.

Hamiltonian, **H**, is given by

$$\Phi_i^{(1)}(\omega) = \sum_R \frac{\langle R|\mu_i|G\rangle}{E_R - E_G + \hbar + i\Gamma}|R\rangle \qquad (2)$$

The first-order NLO coefficients can be expressed as

$$\beta_{ijk}(\omega_1, \omega_2) = P_{ijk}\langle\phi_i^{(1)}(-\omega_1 - \omega_2)|\mu_j|\phi_k^{(1)}(-\omega_1)\rangle \qquad (3)$$

where the *P* operators generate all permutations. This method involves solving for the correction vectors on the basis of the configuration functions. The Hamiltonian matrix, dipole matrix, and overlap matrix are usually constructed on the basis of configuration function, in the CI calculation. In this ZINDO/CV calculation, we have retained all singly and doubly excited configurations generated from the ground-state Slater determination by considering 20 HOMOs and 20 LUMOs. The ZINDO/CV calculation of β thus included all the excited states of the Hamiltonian in the restricted CI space. The average β values are then given by

$$\beta^i_{av} = \sum_{j=1}^{J=3} {}^1/_3(\beta_{ijj} + \beta_{jji} + \beta_{jij}) \qquad (4)$$

The TPA process corresponds to the simultaneous absorption of two photons. The TPA efficiency of an organic molecule, at optical frequency $\omega/2\pi$, can be characterized by the TPA cross sections, $\delta(\omega)$. The TPA cross section is related to the imaginary part of the second hyperpolarizability, $\gamma(-\omega; \omega,\omega, -\omega)$, by[32−35]

$$\delta(\omega) = \frac{3\hbar\omega^2}{2n^2c^2}L^4\{\mathrm{Im}\}\gamma(-\omega; \omega,\omega, -\omega) \qquad (5)$$

where $\hbar$ is the Planck constant divided by 2π, n is the refractive index of the medium, c is the speed of light, L is a local field factor (equal to 1 for vacuum). ZINDO/CV methodology is adapted here to calculate the second hyperpolarizabilities.

The standard expression for the (*ij*)th component of the transition matrix element for TPA to the state $|2A\rangle$ is given by[33−36]

$$s_{ij}(\omega) = \sum_R \left[\frac{\langle G|\mu_i|R\rangle\langle R|\mu_j|2A\rangle}{E_R - E_G - \omega} + \frac{\langle G|\mu_j|R\rangle\langle R|\mu_i|2A\rangle}{E_R - E_G - \omega} \right] \quad (6)$$

The above expression can be rewritten using the first-order CV

$$s_{ij} = \langle \phi_i^{(1)}(-\omega)|\mu_j|2A\rangle + \langle \phi_j^{(1)}(-\omega)|\mu_i|2A\rangle \quad (7)$$

The orientational average of the TPA cross section, $\delta_{TP}(\omega)$, which corresponds to the observed cross section in solutions, is given by[18]

$$\delta_{TP} = \frac{1}{30}\sum_{ij}(2s_{ii}s_{jj}^* + 4s_{ij}s_{ij}^*) \quad (8)$$

In this study, we first optimized the molecular geometries of all considered species at the DFT/PCM level in the presence of an appropriate dielectric for different solvents using the Gaussian 03 package. The optimized DFT level geometry was then used as an input for ZINDO/SCRF/SOS calculation.

To compare with the experimental results, it is necessary to have a cross section in units of (cm^4 s)/photon. The TPA cross section directly comparable with experiment can be defined as

$$\delta_{max} = \frac{4\pi^3 {a_0}^5 \alpha\omega^2 g(\omega)\delta_{TP}}{c\Gamma} \quad (9)$$

where a_0 is the Bohr radius, c is the speed of light, α is the fine structure constant, and $\hbar\omega$ is the photon energy. The factor $(g(\omega)/\Gamma)$ relates the theoretical results to the shape of the exciting laser line defined by the function $g(\omega)$, and $\hbar/\Gamma$ is the lifetime broadening of the final state in atomic units. To make sensible comparison with previous results, Γ is set equal to 0.1 eV and $g(\omega)$ is assumed to be a constant, set equal to 1.

To account for the solvent polarity effect in the ZINDO/CV approach, we have used expanded self-consistent reaction field (SCRF) theory[52] where self-consistent solute/solvent interactions are described by multipolar terms up to $l = 1-12$. According to this procedure, the reaction field, R, can be defined as

$$R = g_l(\epsilon)\langle\psi|M_{lm}|\psi\rangle \quad (10)$$

Where M_{lm} is the moment of the solute charge distribution and the proportional constant g is the modified Onsager factor which can be defined as

$$g_l(\epsilon) = \frac{1}{{a_0}^{2l+1}} \frac{(l+1)(\epsilon-1)}{l+\epsilon(l+1)} \quad (11)$$

For $l = 1$ (dipolar term),

$$g(\epsilon) = \frac{2(\epsilon-1)}{(2\epsilon+1){a_0}^3} \quad (12)$$

where ϵ is the dielectric constant of the solvent and a_0 is the radius of the spherical cavity. To find out the solvent effect for octupolar molecules, here, we have used $l = 1-12$. The cavity radius, as used in this ZINDO/CV/SCRF calculation, was obtained from the DFT method by calculating the radius, b, from the molecular volume ($=4b^3/3\Pi$) first and then adding 0.5 Å to account for the nearest approach of the solvent molecules. In other words, a_0 was taken as $(b + 0.5)$ Å. To avoid the dispersion effect, we have used a photon wavelength corresponding to 1560 nm for computing β tensors. Kanis et. al have shown[48,49] that ZINDO/SCRF can reproduce experimental results in donor−acceptor organic molecules reasonably well. In the above case, we first optimized the geometry at the DFT/PCM level in the presence of an appropriate dielectric for different solvents using the Gaussian 03 package. The optimized DFT level geometry is then used as an input for ZINDO/SCRF/CV calculation at a photon wavelength corresponding to 1560 nm.

TABLE 1: Theoretical (ZINDO/CV/SCRF) Dynamic First Hyperpolarizabilities (in 10^{-30} esu) for Compounds 1a and 1b with Different Donors−Acceptors[a]

donor	$\langle\beta_{zzz}^{1a}\rangle$	$\langle\beta_{zzz}^{1b}\rangle$	$\langle\beta_{exp}^{1a}\rangle$[b]
NMe_2	96	42	35
piperidyl	84	36	25
OMe	55	26	
Me	40	19	
F	44	21	

[a] The conversion factor for β values is 1×10^{-30} esu $= 371.1 \times 10^{-53}$ C^3 m^3 $J^{-2} = 115.74$ au. [b] Experimental data has been taken from ref 14.

TABLE 2: Theoretical (ZINDO/CV/SCRF) Two-Photon Absorption Cross Section (in 10^{-50} (cm^4 s)/Photon) for Compounds 1a and 1b with Different Donors−Acceptors

donor	$\langle\delta_{max}^{1a}\rangle$	$\langle\delta_{max}^{1b}\rangle$	$\langle\delta_{max}^{1b}\rangle$[a]
NEt_2	580	248	197
NPh2	890	360	295
OMe	410	180	
Me	305	110	
F	328	130	

[a] Experimental data has been taken from ref 38.

Results and Discussion

Effect of Donor or Acceptor Substitution. Dynamic hyperpolarizabilities and TPA cross sections of 1,3,5-substituted benzenes and triazines calculated by the ZINDO/CV/SCRF method are listed in Tables 1 and 2. Experimental data[14] for neutral compounds are also displayed in Tables 1 and 2. The comparison of the magnitudes of the molecular first-order hyperpolarizabilities obtained from hyper-Rayleigh scattering (HRS) studies[53] does not require the computation of β projected onto the dipole moment, μ, since the orientation averaged value is the relevant parameter and is evaluated directly. In a HRS experiment,[53] one measures average $\langle\beta^2\rangle$ for any molecule, where

$$\langle{\beta_{HRS}}^2\rangle = \langle{\beta_{ZZZ}}^2\rangle + \langle{\beta_{XZZ}}^2\rangle \quad (13)$$

For an octupolar molecule with C_3, D_3, or D_{3h} symmetry,

$$\langle{\beta_{ZZZ}}^2\rangle = 24/105\,{\beta_{zzz}}^2 \quad (14)$$

and

$$\langle{\beta_{XZZ}}^2\rangle = 16/105\,{\beta_{zzz}}^2 \quad (15)$$

though in the HRS expression an isotropic average is made for all of the molecule β tensor components, indicating that the HRS is sensitive to all such contributions. However, for octupolar molecules, only the $\langle\beta_{zzz}\rangle$ tensor contributes to the total β. Our calculated β_{zzz} and TPA cross-section values match

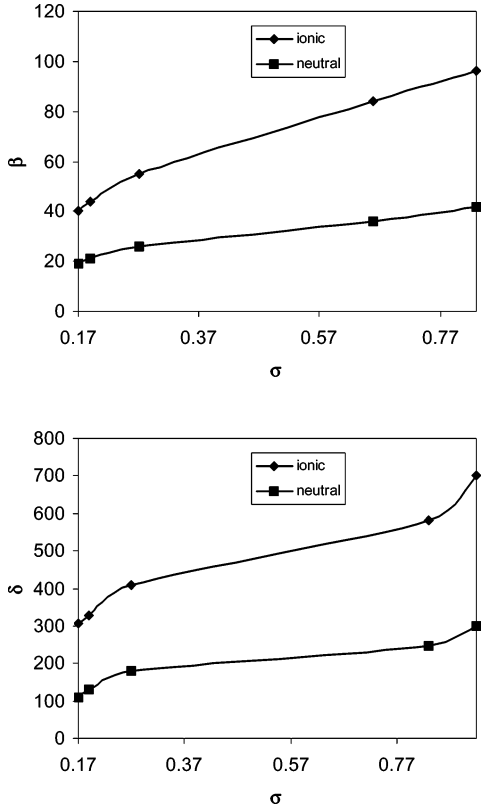

Figure 3. (a) Plot of β_{zzz} vs σ for compounds **1a** and **1b**. (b) Plot of δ_{max} vs σ for compounds **1a** and **1b**.

very well with the experimental values,[14,38] as shown in Tables 1 and 2. The trends in hyperpolarizabilities and TPA cross section with the change of substituents follow the variations of the Hammett parameter constant, σ_p, as we can see from Figure 3. It is interesting to note that both β_{zzz}'s and δ_{max} for ionic octupolar chromophores are 2−4 times larger than those for the corresponding neutral molecules. The quadratic hyperpolarizability of a D_{3h} symmetric molecule can be approximated by a three-level model,[8−11] as shown below,

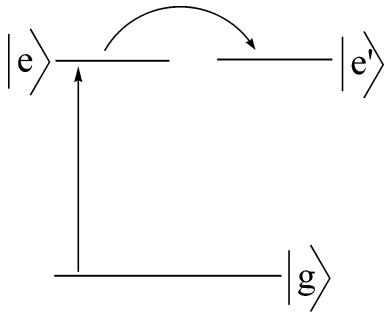

and

$$\beta_{zzz} = \frac{4\pi^2}{\hbar^2} \times \frac{\mu_{ge}^2 \mu_{ee'}}{\omega_{ge}^2} \times \frac{\omega_{ge}^2}{(\omega_{ge}^2 - 4\omega^2)(\omega_{ge}^2 - \omega^2)} \quad (16)$$

static factor dispersion factor

where μ_{ge}^2 denotes the square of the transition moment between ground and degenerate excited charge-transfer (CT) states, $\mu_{ee'}$ is the transition moment connecting these degenerate excited states, ω_{ge} is the CT energy, and ω is the fundamental energy of the incident light. The energy gap between the ground and 2-fold degenerate excited states monotonically decreases, and the transition dipole elements monotonically increase with the increase of the Hammett parameter constant for donor and also as we move from a neutral to an ionic system for the same donor groups.

Zojer et. al.[32] have discussed in detail how one can use the three-level model for calculating the TPA cross sections of nondipolar molecules. For octupolar molecules, the TPA cross section can be defined as[33−35]

$$\delta_{3\text{-state}} = K_2 \frac{L^4}{n^2 c^2 \epsilon_0 \hbar} (E_{ge'}/2)^2 \frac{M_{ge}^2 M_{ee'}^2}{(E_{ge} - E_{ge'}/2)^2 \Gamma} \quad (17)$$

where K_2 is a numerical factor, whose actual value depends on the relative orientation of the change in state dipole and the transition dipole moments. M_{ge} and $M_{ee'}$ are the transition dipoles between the ground-state $|g\rangle$, an intermediate state $|e\rangle$ and between $|e\rangle$, $|e'\rangle$, respectively. E_{ge} and $E_{ge'}$ are the corresponding transition energies. i and j refer to the Cartesian coordinates. $E_{ge'}$ is the excitation energy at the peak of the two-photon absorption band, n is the refrective index of the solvent, and L is the local field factor. The results of our calculation indicate that, as the charge-transfer character of the ground electronic state (as shown in Figure 2c) increases by increasing the strength of donor and acceptor, (i) both the energy gap between the degenerate first excited states and the ground state as well as the target TPA state and the ground state decrease, (ii) the energy gap difference $E_{ge} - E_{ge'}$ decreases, and consequently (iii) the product of transition dipole matrix elements $|M_{ge}M_{ee'}|$ amplitude monotonically increases.

Chain Length Dependence of NLO Properties and TPA Cross Sections. Elongation of the conjugation pathway is one of the primary design steps for increasing β values of neutral and ionic dipolar organic molecules, and several studies have been performed to obtain insight into this phenomenon.[1−8] However, to the best of our knowledge, there are very few reports on the relevant studies for the octupolar molecules. We have applied the DFT/6-31G**/PCM scheme using $CHCl_3$ solvent to optimize the structure of compounds **2a** and **2b** with NEt_2 donor and the ZINDO/CV/SCRF method to calculate their dynamic β vales with the increment of the number of double bonds from 2 to 5. The optimized geometry of all the molecules is characterized by C_3 symmetry. Harmonic vibrational frequency analysis indicates that all the structures are minima on the potential energy surface. Figure 4a shows how the first hyperpolarizability increases with the elongation of the chain lengths. Our data indicate a significant increase in the first hyperpolarizability on elongation on the conjugation pathway. β increases 1.6 times as the number of conjugated double bonds increase from 1 to 2. Though the trend in β_{zzz} versus n for both series is the same, always for a given number of π bonds (n values), the dynamic first hyperpolarizabilities of the ionic octupoles are much higher than those for the corresponding neutral octupoles. It is interesting to note that β for both ionic and neutral chromophores peaks at $n = 5$ and then starts decreasing. Our calculations indicate a saturation limit of octupolar β at $n = 5$.

It is known in the literature that the second hyperpolarizability of a conjugated polyene molecule increases as the chain length increases.[1−5] Since TPA cross section is related to the imaginary part of the second hyperpolarizability, one can expect that the TPA cross section will follow a similar pattern. Figure 4b shows how the TPA absorption cross sections increase with the elongation of the chain lengths. Our data indicate a significant

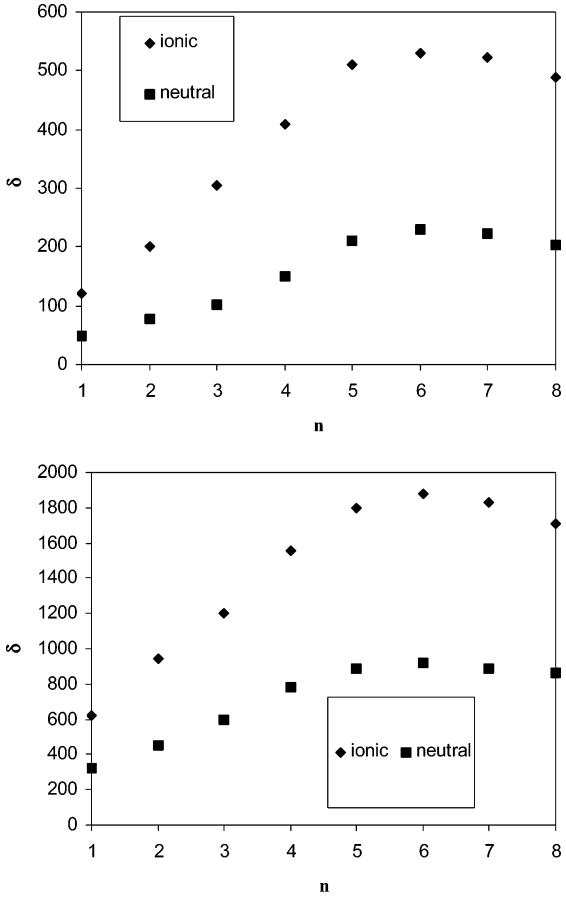

Figure 4. (a) Plot of β_{zzz} vs n for compounds **2a** and **2b**. (b) Plot of δ_{max} vs n for compounds **2a** and **2b**.

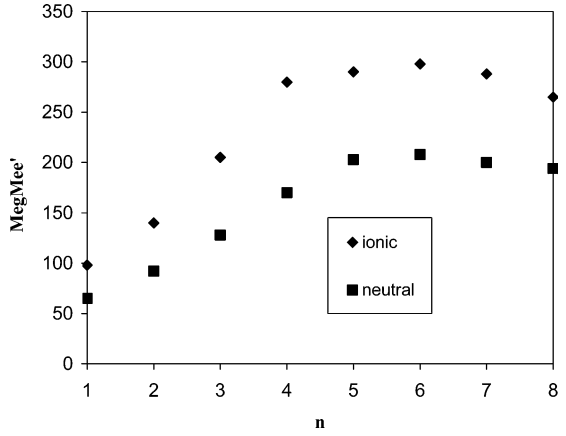

Figure 5. $|M_{ge}M_{ee'}|$ vs n for compounds **2a** and **2b**.

increase in the TPA cross section on elongation of the conjugation pathway. δ_{max} increases 1.45 times as the number of conjugated double bonds increases from 1 to 2. As the chain length increases, the energy differences, both E_{ge} and $E_{ge'}$, decrease and the oscillator strength increases. The TPA cross sections for the ionic octupoles are much higher than those for the corresponding neutral octupoles. It is surprising to note that our calculations indicate a saturation phenomena above $n = 5$. We have seen same saturation behavior for first hyperpolarizabilities above $n = 5$. To understand the saturation behavior, we have plotted $|M_{ge}M_{ee'}|$ versus n (number of double bonds), as shown in Figure 5. Figure 5 indicates that the product of transition dipole matrix elements also follows the same trend as we have noted for the β and TPA cross sections. We believe

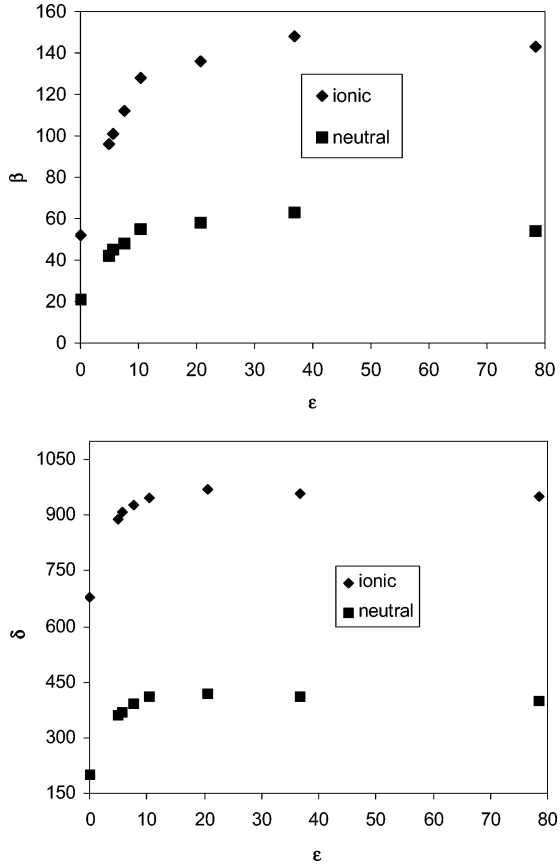

Figure 6. (a) Plot of β vs ϵ for compounds **1a** and **1b**. (b) Plot of δ vs ϵ for compounds **1a** and **1b**.

that the transition matrix dipole is largely responsible for the above saturation behavior.

Solvent Effect. It is now well-known that the solvent polarity exerts an important influence on the structure as well as the first NLO coefficients in the dipolar molecules.[1−10,23,24] Due to the lack of a permanent dipole moment in octupolar molecules, one can assume that these molecules will show little solvent dependent hyperpolarizabilities. We have shown recently that the common notion may not be valid for benzene-substituted octupolar molecules. To find out whether the same fact is valid for this series of octupolar molecules or not, we optimized the geometry using the SCRF/PCM approach and the dynamic NLO properties are calculated with the ZINDO/CV/SCRF method. Figure 6a shows the evolution of first hyperpolarizabilitity as a function of dielectric constant, ϵ. Our calculation indicates that the β value first increases rapidly as we move from the gas phase to solvent media with increasing ϵ, then decreases, and then finally saturates at above $\epsilon = 20$. This suggests that the solvent reaction field interaction with the octupolar chromophore through quadrupolar, octopolar, and higher-order moments could be the dominant contribution to the solvent process. Our calculations indicate that more than 80% of the contribution arises due to the interaction from quadrupolar and octupolar moments and higher-order moments turn out not to be very much significant. This solvent effect is due to the fact that the degree of charge delocalization increases as the solvent polarity or solvent dielectric constant increases. This observation with saturation above $\epsilon = 15-20$ is in agreement with the reported result by Dehu et al.[55] and Luo et al.[56] for neutral octupolar systems.

The δ_{max} values for the ionic octupolar chromophores are always higher in any solvent than that of the corresponding

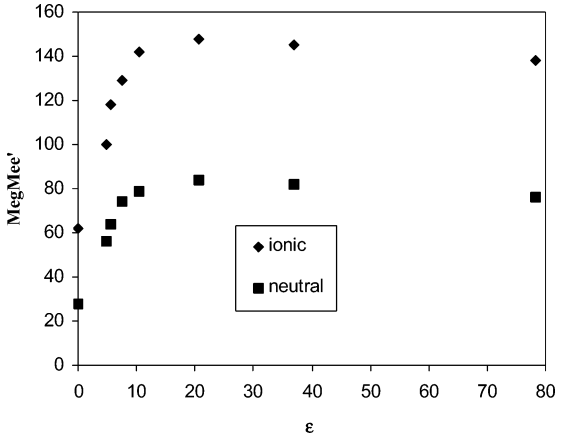

Figure 7. $|M_{ge}\ M_{ee'}|$ vs ϵ for compounds **1a** and **1b**.

neutral chromophores. The solvent dependence of the TPA cross section is shown in Figure 6b. Though solvent plays a significant role in the TPA properties, the solvent dependence is found to be smaller than that of β_{zzz}. Figure 6b displays a saturation phenomenon for δ_{max}, for the solvents with $\epsilon > 20$, and the trend is similar to that of the first hyperpolarizabilities. Similar trends have also been noted by Luo et al.[41] for the dipolar molecules. To understand the saturation behavior, we have calculated $|M_{ge}M_{ee'}|$ values at different ϵ values, as shown in Figure 7. Our calculation indicates that the product of transition matrix elements also follows the same trend as we have noted for the β and TPA cross sections. We believe that the transition matrix product is largely responsible for the above saturation behavior.

Conclusion

In this paper, we have reported the first hyperpolarizabilities and TPA cross sections of the ionic octupolar chromophores and compared their values with those of neutral octupoles. We have analyzed a variety of effects on the β and δ_{max} values for ionic octupolar molecules including the relationship between TPA cross sections, the first hyperpolarizability, and the donor−acceptor properties and the influence of solvent polarity and conjugation length. It is found that, as the strength of the donor and acceptors increases, (i) the energy gap between degenerate first excited electronic states and the ground electronic state decreases and (ii) the product of transition dipole matrix elements increases. The calculated β and δ_{max} values for neutral chromophores are comparable with the experimental data wherever available. We have demonstrated that the dynamic hyperpolarizabilities and δ_{max} for ionic chromophores are several times higher than those of neutral octupolar molecules, and it is due to the fact that (i) both the energy gap between the degenerate first excited states and the ground state as well as the target TPA state and the ground state decrease as we move from neutral to ionic octupoles with the same donor and acceptor and (ii) the product of transition dipole matrix elements is much higher for ionic octupolar molecules than for the corresponding neutral ones. We find that the solvents play a significant role in the first hyperpolarizabilities and δ_{max} of ionic and neutral octupolar molecules. Interestingly, both properties display a maximum value at $\epsilon \approx 20$ and then decrease slowly. Our calculation indicated that the product of transition matrix elements also follows the same trend. The solvent chain length dependence of the two-photon absorption, first hyperpolarizabilities display a saturation behavior at $n = 5$, and we have found that the product of transition matrix elements is largely responsible for the saturation behavior.

Acknowledgment. We thank the NSF-CREST (grant HRD-0318519) and ONR (grant no. N00014-03-1-116) for generous funding. We also thank Mississippi Center for Super Computer Resource (MCSR), University of Mississippi, Oxford, MS, for the generous use of their computational facilities and the reviewers whose valuable suggestions improved the quality of the manuscript.

References and Notes

(1) Zyss, J. *Molecular Nonlinear Optics: Materials, Physics and Devices*; Academic Press: New York, 1994.
(2) Nalwa, H. S., Miyata. S., Ed. *Nonlinear Optics of Organic Molecules and Polymers*; CRC Press: Boca Raton, FL, 1997.
(3) Mkuzyk, M. G. *Nonlinear Optical Properties of Organic Materials*; SPIE Proceedings, 1997; 3147.
(4) Marder, S. R.; Perry, J. W.; Schaefer, P. W. *Science* **1989**, *245*, 626.
(5) Clays, K.; Wostyn, K.; Olbrechtes, G.; Persoons, A.; Watanabe, A.; Nogi, K.; Duan, X.-M.; Okada, S.; Oikawa, H.; Nakanishi, H.; Bredas, J. L. *J. Opt. Soc. Am. B* **2000**, *17*, 256.
(6) Clays, K.; Coe, B. *J. Chem. Mater.* **2003**, *15*, 642.
(7) Coe, B. J.; Jones, L. A.; Harrs, J. A.; Brunschwig, B. S.; Asselberghs, I.; Clays, K.; Persoons, A. *J. Am. Chem. Soc.* **2003**, *125*, 862.
(8) Coe, B. J.; Jones, L. A.; Harrs, J. A.; Brunschwig, B. S.; Asselberghs, I.; Clays, K.; Persoons, A.; Garin, J.; Orduna, J. *J. Am. Chem. Soc.* **2004**, *126*, 3880.
(9) Zyss, J.; Ledoux, I. *Chem. Rev.* **1994**, *94*, 77.
(10) Zyss, J. *Nonlinear Opt.* **1991**, *1*, 3.
(11) Zyss, J. *J. Chem. Phys.* **1993**, *98*, 6583.
(12) Ledoux, I.; Zyss, J.; Siegel, J.; Brienne, J.; Lehn, J. M. *Chem. Phys. Lett.* **1990**, *440*, 172.
(13) Ray, P. C.; Das, P. K. *Chem. Phys. Lett.* **1995**, *244*, 153.
(14) Chao, B. R.; Park, S. B.; Lee, S. J.; Son, K. H.; Lee, S. H.; Kang, T. I.; Cho, M.; Jeon, S. J. *J. Am. Chem. Soc.* **2001**, *123*, 6421.
(15) Senechal, K.; Maury, O.; Ledoux, I.; Zyss, J. *J. Am. Chem. Soc.* **2002**, *124*, 4560.
(16) McDonagh, A. M.; Humphrey, M. G.; Samoc, M.; Luther-Davies, B.; Houbrechts, S.; Wada, T.; Sasbe, H.; Persoons, A. *J. Am. Chem. Soc.* **1999**, *121*, 1405.
(17) Bartholomew, G. P.; Ledoux, I.; Mukamel, S.; Bazan, G. C.; Zyss, J. *J. Am. Chem. Soc.* **2002**, *124*, 13480.
(18) Hennrich, G.; Asselberghs, I.; Clays, K.; Persoons, A. *J. Org. Chem.* **2004**, *69*, 5077.
(19) Stadler, S.; Brauchle, Ch.; Brandl, S.; Gompper, R. *Chem. Mater.* **1996**, *8*, 676.
(20) Luo, Y.; Cesar, A.; Agren, H. *Chem. Phys. Lett.* **1996**, *252*, 389.
(21) Zhu, W.; Wu, G.-S. *J. Phys. Chem. A* **2001**, *105*, 9568.
(22) Ray, P. C. *Chem. Phys. Lett.* **2004**, *394*, 354.
(23) Ray, P. C. *Chem. Phys. Lett.* **2004**, *395*, 269.
(24) Ray, P. C.; Leszczynski, J. *Chem. Phys. Lett.* **2004**, *399*, 162.
(25) Van Stryland, E. W.; Wu, Y. Y.; Hagan. D. J.; Soileau, M. J.; Mansour, K. *J. Opt. Soc. Am. B* **1988**, *5*, 1980.
(26) Mukherjee, A. *Appl. Phys. Lett.* **1993**, *62*, 3423.
(27) Wang, X.; Kerbs, L. J.; Pudavar, H. E.; Ghosal, S.; Liebow, C.; Schally, A. V.; Prasad, P. N. *Proc. Natl. Acad. Sci. U.S.A.* **1999**, *96*, 11081.
(28) Joshi, M. P.; Pudavar, H. E.; Swaitkiewicz., J.; Prasad, P. N.; Reianhardt, B. *Appl. Phys. Lett.* **1999**, *74*, 170.
(29) Kawatta, S.; Kawatta, Y. *Chem. Rev.* **2000**, *100*, 1777.
(30) Bauer, C.; Schnabel, B.; Kley, E. B.; Scherf, U.; Giessen, H.; Mahrt, R. F. *Adv. Mater.* **2002**, *14*, 673.
(31) Spangler, C. W. *J. Mater. Chem.* **1999**, *9*, 2013.
(32) Zhou, W. H.; Kuebler, S. M.; Yu, T. Y.; Ober, C. K.; Perry, J. W.; Marder, S. R. *Science* **2002**, *196*, 1106.
(33) Zojer, E.; Wenseleers, W.; Pacher, P.; Barlow, S.; Halik, M.; Grasso, C.; Perry, J. W.; Marder, S. R.; Bredas, J. L. *J. Phys. Chem. B* **2004**, *108*, 8641.
(34) Masunov, A.; Tretiak, S. *J. Phys. Chem. B* **2004**, *108*, 899.
(35) Beljonne, D.; Wenseleers, W.; Zojer, E.; Shuai, Z.; Pond, S. J. K.; Perry, J. W.; Marder, S. R.; Bredas, J. L. *Adv. Funct. Mater.* **2002**, *12*, 631.
(36) Pati, S. K.; Marks, T. J.; Ratner, M. A. *J. Am. Chem. Soc.* **2001**, *123*, 7287.
(37) Kannan, R.; Guang, He.; Prasad, P. N..; Vaia, R. A.; Tan, L. S. *Chem. Mater.* **2004**, *16*, 185.

(38) Cho, B. R.; Son, K. H.; Lee, S. H.; Song, Y. S.; Lee, Y. K.; Jeon, S. J.; Lee, H.; Cho, M. *J. Am. Chem. Soc.* **2001**, *123*, 10039.
(39) Zalesny, R.; Bartkowiak, W.; Styrcz, S.; Leszczynski, J. *J. Phys. Chem. A* **2002**, *106*, 4032.
(40) Jha, P. C.; Das, J. M.; Ramasesha, S. *J. Phys. Chem. A* **2004**, *108*, 6279.
(41) Luo, Y.; Norman, P.; Macak, P.; Agren, H. J. *Phys. Chem. A* **2000**, *104*, 4718.
(42) Wang, C. K.; Zhao, K.; Su, Y.; Ren, Y.; Zhao, X.; Luo, Y. *J. Chem. Phys*. **2003**, *19*, 1208.
(43) Werts, M. H. V.; Gmouh, S.; Mongin, O.; Pons, T.; Blanchard-Desce, M. *J. Am. Chem. Soc.* **2004**, *126*, 16294.
(44) Glenn, P. B.; Rumi, M.; Pond, S. J. K.; Perry, J. W.; Tretiak, S.; Bazan, G. C. *J. Am. Chem. Soc.* **2004**, *126*, 11529.
(45) Mennucci, B.; Tomasi, J. *J. Chem. Phys.* **1997**, *106*, 5151.
(46) Frisch, M. I.; Trucks, G. W.; Schlegel, H. B.; Pople, J. A. *Gaussian 03*, revision A11; Gaussian Inc.: Pittsburgh PA, 2003.
(47) Kotzian, M.; Rosch, N.; Schroder, H.; Zerner, M. C. *J. Am. Chem. Soc.* **1989**, *111*, 7687.
(48) Kanis, D. R.; Ratner, M. A.; Marks, T. J. *J. Am. Chem. Soc*. **1993**, *115*, 1078.
(49) Kanis, D. R.; Lacroix, P. G.; Ratner, M. A.; Marks, T. J. *J. Am. Chem. Soc*. **1994**, *116*, 10089.
(50) Ramasesha, S.; Shuai, Z.; Bredas, J. L. *Chem. Phys. Lett.* **1995**, *245*, 226.
(51) Ray, P. C.; Ramasesha, S.; Das, P. K. *J. Chem. Phys*. **1996**, *105*, 9633.
(52) Rivali, J. L.; Rinaldi, D. *Chem. Phys*. **1976**, *18*, 233.
(53) Hendrickx, E.; Clays, K.; Persoons, A. *Acc. Chem. Res.* **1998**, *31*, 675.
(54) Bartkowiak, W.; Zaslesny, R.; Niewodniczanski, W.; Leszczynski, J. *J. Phys. Chem. A* **2001**, *105*, 10702.
(55) Dehu, C.; Geskin, V.; Persoons, A.; Bredas, J. L. *Eur. J. Org. Chem.* **1998**, 1267.
(56) Luo, Y. *J. Am. Chem. Soc*. **1998**, *120*, 11188.